Nuclear Engineering and Technology 52 (2020) 1626–1637

Contents lists available at ScienceDirect

Nuclear Engineering and Technology

journal homepage: www.elsevier.com/locate/net

Original Article

Application case for phase III of UAM-LWR benchmark: Uncertainty propagation of thermal-hydraulic macroscopic parameters

C. Mesado, R. Miró, G. Verdú*

Institute for the Industrial, Radiophysical and Environmental Safety (ISIRYM), Universitat Politècnica de València, 46022, Valencia, Spain

ARTICLE INFO

Article history:
Received 20 August 2019
Received in revised form
26 December 2019
Accepted 12 January 2020
Available online 18 January 2020

Keywords:
UAM benchmark
U&S analysis
Uncertainty propagation
3D vessel
TRACE
PARCS
RESTING

ABSTRACT

This work covers an important point of the benchmark released by the expert group on Uncertainty Analysis in Modeling of Light Water Reactors. This ambitious benchmark aims to determine the uncertainty in light water reactors systems and processes in all stages of calculation, with emphasis on multi-physics (coupled) and multi-scale simulations. The *Gesellschaft für Anlagen und Reaktorsicherheit* methodology is used to propagate the thermal-hydraulic uncertainty of macroscopic parameters through TRACE5.0p3/PARCSv3.0 coupled code. The main innovative points achieved in this work are i) a new thermal-hydraulic model is developed with a highly-accurate 3D core discretization plus an iterative process is presented to adjust the 3D bypass flow, ii) a control rod insertion occurrence —which data is obtained from a real PWR test— is used as a transient simulation, iii) two approaches are used for the propagation process: *maximum response* where the uncertainty and sensitivity analysis is performed for the maximum absolute response and *index dependent* where the uncertainty and sensitivity analysis is performed at each time step, and iv) RESTING MATLAB code is developed to automate the model generation process and, then, propagate the thermal-hydraulic uncertainty. The input uncertainty information is found in related literature or, if not found, defined based on expert judgment. This paper, first, presents the *Gesellschaft für Anlagen und Reaktorsicherheit* methodology to propagate the uncertainty in thermal-hydraulic macroscopic parameters and, then, shows the results when the methodology is applied to a PWR reactor.

1. Introduction

This work covers one of the main phases of the benchmark released by the expert group on *Uncertainty Analysis in Modeling of Light Water Reactors* (UAM-LWR). The UAM benchmark [1] was born in 2006 at the University of Pisa (Italy) due to the need of best estimate calculations together with its confidence bounds. Thus, the UAM expert group aims to obtain the current state and future needs of *Uncertainty and Sensitivity* (U&S) analysis in modeling, with emphasis on multi-physics (coupled) and multi-scale simulations. With this information, the benchmark main goal is to determine the uncertainty in LWR systems in all stages of calculation. The benchmark is subdivided into three phases:

1. Neutronic phase: multi-group microscopic and macroscopic cross-section library and criticality analyses.
2. Core phase: stand-alone thermal-hydraulic and neutronic codes.
3. System phase: coupled thermal-hydraulic and neutronic code.

To establish proper confidence bounds an *Uncertainty Quantification* (UQ) method must be used. There are several UQ methods, however, one of the most used method in the nuclear field, and also recommended by the UAM benchmark organizers, is the *Gesellschaft für Anlagen und Reaktorsicherheit* (GRS). The GRS method is widely used in the literature, for example [2]. The main advantage of GRS is that it is easy to implement, the downside is that *Probability Distribution Function* (PDF) for input parameters must be based on expert judgment if no experimental information is available, this could lead to biased information. Besides, this method usually requires significant computational cost. When using the GRS methodology, the user must be aware of a few things:

1. A range and a PDF for each uncertain input parameter must be identified. Ideally, the PDFs should be obtained using

* Corresponding author.
E-mail address: gverdu@iqn.upv.es (G. Verdú).

https://doi.org/10.1016/j.net.2020.01.010

Nomenclature

α	Quantile
β	Probability or confidence level
ε	Wall roughness
ε_{by}	Flow tolerance limit
χ^2	Inverse chi-squared CDF
A_{by}	Flow area
CHFM	Critical heat flux multiplier
Cp_{fuel}	Fuel heat capacity
Cp_{clad}	Clad heat capacity
D_{hyd}	Hydraulic diameter
Flow_{by}	Simulated bypass flow
$\text{Flow}^*_{\text{by}}$	Theoretical bypass flow
h_{gap}	Gap heat transfer coefficient
i	Iteration index
k	Wilks' order
k_{fac}	Grid friction factors
K^Z_{by}	Axial bypass friction coefficient
K^R_{by}	Radial bypass friction coefficient
K_{clad}	Fuel thermal conductivity
K_{fuel}	Clad thermal conductivity
m_{in}	Inlet mass flow
n	Sample size
n_{assm}	Fuel assemblies
n_t	Theta sectors in cylindrical vessel
n_x	Cartesian vessel cells in x axis
n_y	Cartesian vessel cells in y axis
n_z	Cartesian vessel cells in z axis
p/d	Pitch to diameter ratio
P_{out}	Output pressure
q_{byp}/q_{tot}	Bypass heat fraction
q_{mod}/q_{tot}	Moderator heat fraction
r	Dependent responses
r_s	Critical correlation value
RFPF	Radial fuel peaking factor
s	One or two-sided tolerance region
t_s	Inverse t-Student CDF
T_{in}	Inlet flow temperature
z	Upper critical value
z_{gap}	Gap size

experimental data. However, in reality such data is commonly not available. In such cases, it is common to assign a uniform or normal distribution [3], otherwise expert judgment is used to assign a range and PDF. Nevertheless, the use of expert judgment is often unreal and should be used with caution.

2. The uncertain input parameters are sampled n times, there are several sampling techniques that can be used. Being the most common the *Simple Random Sampling* (SRS) −expensive method since the n must be high compared to other methods to obtain the same coverage−, *Stratified Sampling* with a better coverage and *Latin Hypercube Sampling* (LHS) with an improvement over the stratified sampling with additional computational cost to reduce the bias. It is known that more accurate model response variance is obtained using LHS [4], but results differences are not significant [5].
3. Parametric or non-parametric samplings are possible to obtain the number of samples or code runs, n. The number of samples could be greatly reduced using a non-parametric sampling because all uncertain parameters are sampled at the same time. Therefore, with non-parametric sampling, the number of runs depends only on the tolerance and confidence interval of responses. That implies that the number of input parameters involved do not have any limitation. Moreover, in a parametric sampling the hypothesis for normality must be checked, while in non-parametric samplings any distribution could be assumed.

The determination of the minimum sample runs, n, is important. For a non-parametric approach, the parameter n is such that when the code is run n times −or samples−, the response of interest will meet a certain tolerance limit (required a priori). The method to obtain n with a certain quantile, α, and a probability or confidence level, β, was developed by Wilks ([6,7]). The formula for one-sided tolerance region ($s = 1$) is given by Eq (1) and Eq (2) for first and second order (k) respectively. For example, for a one-sided 95/95 tolerance region, a minimum sample size of 59 is obtained if $k = 1$, but the sample size increases to 93 if $k = 2$. The same sample size (93) is obtained if $k = 1$ but a two-sided 95/95 tolerance region is specified (as suggested in Ref. [8]). However, in a recent study ([9,10]) the recommended minimum sample size for the same conditions ($k = 1$ and two-sided) increases to 146 according to Eq (3), where ${}_nC_j$ is the number of combinations of n items taken j at a time. Finally, if there are several dependent responses (r), the minimum sample size increases as given in Eq (4) for $k = 1$, see Refs. [11,12]. For three dependent responses, one-sided 95/95 tolerance region and $k = 1$, the sample size is **124**.

$$1 - \alpha^n \geq \beta \tag{1}$$

$$1 - \alpha^n - n(1-\alpha)\alpha^{(n-1)} \geq \beta \tag{2}$$

$$1 + \alpha^n - 2\alpha^n \sum_{j=0}^{n} {}_nC_j \left(\frac{1-\alpha}{2\alpha}\right)^j \geq \beta \tag{3}$$

$$\sum_{j=0}^{n-s\cdot r} {}_nC_j \, \alpha^j (1-\alpha)^{(n-j)} \geq \beta \tag{4}$$

4. High-fidelity model vs surrogate model. For complex models, if a high fidelity model is used to propagate the uncertainty, the computational effort could be prohibitive. In this case, the high-fidelity or full model can be replaced by a surrogate model. The surrogate model represents the same physical scenarios but it runs simulations faster at expenses of accuracy and range of applicability. In this sense, CSAU methodology replaced TRACE by a surrogate response surface to reduce computational cost.

GRS makes use of a non-parametric sampling, the high-fidelity model and the Wilks' formula to obtain n. The U&S analysis can be obtained with any statistical software available in the market, for example DAKOTA developed at Sandia National Laboratory. It is able to perform UQ (average responses, standard deviations, confidence intervals …). In addition to this information, DAKOTA calculates *Sensitivity Analysis* (SA) by means of sensitivity coefficients assuming linear −*Simple Correlation Coefficient* (SCC) and *Partial Correlation Coefficient* (SCC)− and non-linear relationships

–*Spearman's Rank Correlation Coefficient* (SRCC) and *Partial Rank Correlation Coefficient* (PRCC). Correlation coefficients and other relevant information can be found in Ref. [13].

A critical correlation value (r_s) can be defined as the minimum value for which a parameter is considered to be sensitive –with respect to other parameter–. This value can be calculated according to Eq (5), where n is the number of samples and z is the abscissa over the *Probability Distribution Function* (PDF) that yields a certain quantile –also known as upper critical value–. The absolute value of r_s, between an input and output parameter, gives the minimum value for which the output parameter can be considered sensitive to a variation in the input parameter. For example, with a confidence interval of 95% –commonly accepted value in most fields–, for normal distributions $z = 1.96$, and if n is 146, then $r_s = \pm 0.1628$.

$$r_s = \pm \frac{z}{\sqrt{n-1}} \tag{5}$$

Other confidence intervals could be used, leading to different critical correlation values and, thus, modifying what variables are considered sensitive. Nonetheless, sensitivity ranking of parameters remains constant. In this work $r_s = \pm 0.1628$ is used.

1.1. Overview

This paper presents a methodology to propagate the uncertainty of thermal-hydraulic parameters and has been divided into five sections. The current section introduces the UAM benchmark and GRS methodology. The second section gives an explanation of models used in this work. Section 3 and Section 4 detail the methodology and results for the uncertainty propagation. Finally, the last section, states, briefly, the conclusions.

Due to the high number of data generated in this work, only the most representative results are shown in this paper which intends to show the different possibilities of the methodology. The reader is referred to Ref. [14] to obtain the complete spectrum of results.

2. Models

There are two different models: a thermal-hydraulic model (with TRACE5.0p3 code) and a core model (with PARCSv3.0 code). In this work, the recent tendency to extend codes or models into a 3D discretization is followed regarding the thermal-hydraulic model. It is worth to mention that an effort is made to obtain a highly realistic PWR core model with a 3D discretization –especially cross-flow calculations assessed in Ref. [15]– with TRACE5.0p3. To this end, vessels components are used, these are able to solve the mass and energy balances in 3D. It is seen that the bypass flow in a 3D model fluctuates abruptly over the axial axis due to realistic cross flow simulation. Therefore, an algorithm is presented to adjust the bypass flow to a theoretical value and within a prefixed tolerance limit. The verification of the thermal-hydraulic model is made comparing the 3D model with a traditional 1D model made with pipe components. It must be said that scripts are programmed to automatically generate the correspondent models using MATLAB, see Ref. [14]. Therefore, it is easy to produce input decks with the confidence that they are already tested.

2.1. Thermal-hydraulic model

A PWR is modeled with TRACE5.0p3, the model has the main advantage that the reactor core is fully discretized in 3D. Therefore, in comparison to traditional models, asymmetric phenomena are better represented using this new feature. A core model is build using TRACE 3D components, specifically one cartesian and one cylindrical vessel. The reader is referred to Ref. [16] for more information about this and other 3D models in TRACE. The main characteristics of this 3D model are presented hereafter.

- There is one cartesian vessel –discretized into n_x, n_y and n_z cells– that represents all fuel assemblies. Assemblies are not collapsed, i.e. one cell corresponds to one fuel assembly. In total, there are n_{assm} assemblies.
- There is one cylindrical vessel with two radial nodes. The innermost node represents the core bypass and the outermost simulates the downcomer, see Fig. 1 (left).
- The cylindrical vessel has $n_z + 2$ axial levels, n_z levels equally distributed as the cartesian vessel plus two additional axial levels representing the upper and lower plenum.
- The cylindrical vessel could be discretized in the theta direction to model different theta sectors, n_t. See Fig. 1 for a vessel with 3 theta cells.
- To establish the axial connection, a mapping assigning assemblies and theta sectors is needed, see Fig. 1 (right). Two mappings are established, one for the inlet connections and another for the outlet connections since one bundle could be connected to different theta sectors at inlet and outlet levels.
- One break component is connected to each theta sector of the downcomer (outer radial node in the cylindrical vessel). Breaks are connected to upper axial levels.
- One fill component is connected to each theta sector of the downcomer –at certain level lower than break connections–.
- Mass flow and temperature boundary conditions are set in each fill component, pressure boundary condition is set in each break component.
- One heat structure is coupled with each fuel assembly (cartesian vessel). Besides, one heat structure is associated with each bypass theta sector (cylindrical vessel).
- The heat transfer between bypass and downcomer (reactor barrel) is modeled through a heat structure with convection boundary condition at both sides.
- One power component heats all heat structures but the heat structures simulating the reactor barrel.
- It is not possible to connect the fill or break component directly to the cylindrical vessel, thus one-cell pipes are used between them.
- In order to connect both vessels, single junctions are used in the axial connections.
- Both vessels are also connected sideways at all levels, one-cell pipes are used.

See Fig. 2 for a simplified model –with three theta sectors– sketched using SNAP tool. The total number of components is detailed in Table 1, and expressed in Eq (6).

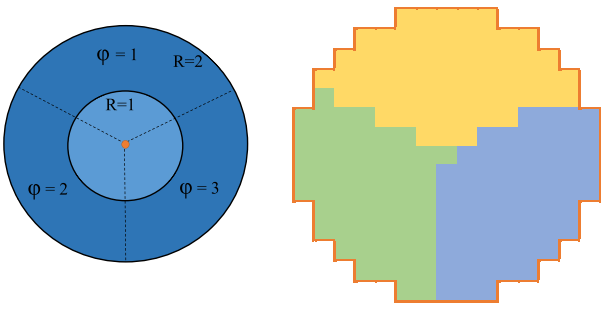

Fig. 1. Cylindrical (left) and cartesian vessel (right).

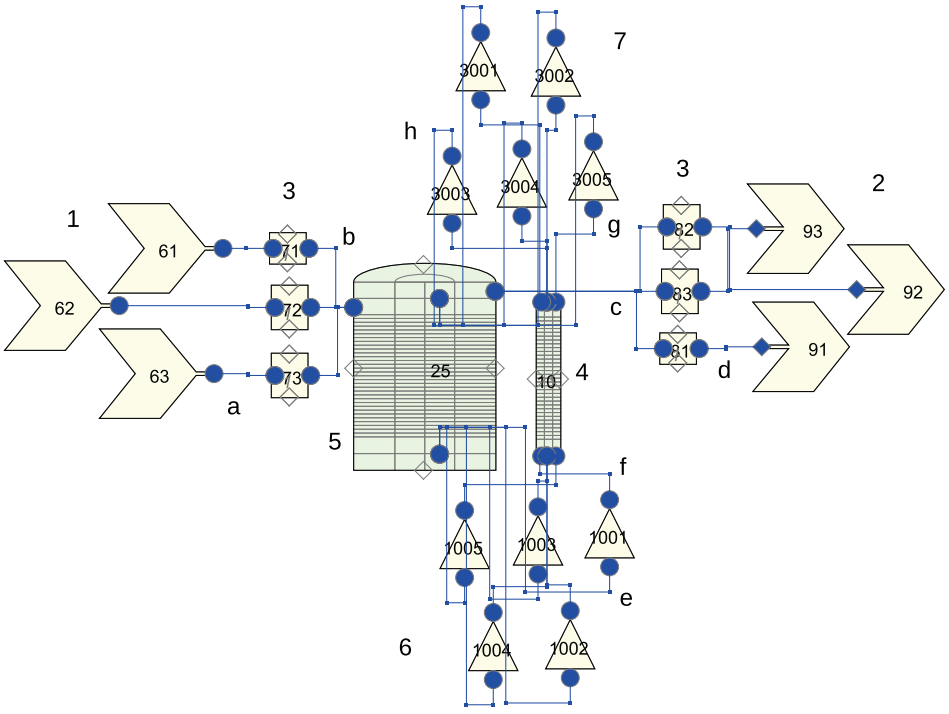

Fig. 2. Simplified thermal-hydraulic model with three theta sectors.

$$n_{comp} = 3 + 6n_t + 3n_{assm} + 2n_z(n_x - 2 + n_y - 2) \quad (6)$$

Where n_t are the theta sectors, n_{assm} is the number of assemblies and n_x, n_y and n_z are the number of cells in each direction of the cartesian vessel. The same can be done with the total number of junctions in the thermal-hydraulic model, Table 2 and Eq (7). The numbers/letters in the first column of Table 1/Table 2 link the components/junctions to the numbers/letters in Fig. 2. Components/junctions without numbers/letters are not displayed in the figure because it is a simplified sketch.

$$n_{junc} = 4\left[n_t + n_{assm} + n_z(n_x - 2 + n_y - 2)\right] \quad (7)$$

In order to verify the 3D model, a traditional 1D model is created in TRACE. It is a model built with 1D pipes and heat structures and without collapsed assemblies. The bypass is modeled using a pipe, also with a heat structure component. All pipes are connected to an upper and lower plenum. The boundary conditions in the fill and break components are the same as in the 3D model, that is, inlet temperature of 568 K, 1.55E7 Pa as output pressure and 5.12E3 kg/s as inlet mass flow. Several plots comparing both models are presented in Fig. 3. It is seen, almost, a perfect agreement between the 1D and the 3D model. It is true that the 3D model uses considerably more computational time, but the main advantage of the 3D model, in comparison of the traditional 1D model, is that it can represent asymmetric phenomena realistically —especially cross-flow among fuel elements and phenomena occurring in the bypass, see Ref. [15].

2.1.1. Bypass flow adjustment

Traditional 1D models do not simulate cross flows, thus the bypass flow is constant with height. Nevertheless, in 3D models, the cross flow exists between reflector zones and fuel assemblies, and also among fuel assemblies. This is especially relevant in the thermal-hydraulic model, where the bypass flow fluctuates strongly not only in the axial axis, but also among theta sectors. This would be a harsh work if it had to be adjusted by hand. Therefore, an iterative process to adjust the bypass flow is developed. The process modifies the bypass friction coefficient until a specified theoretical flow value is reached for all bypass cells. The theoretical flow is a user input parameter, therefore, it must be given either by the power plant or read from SIMULATE output file.

The first iteration starts with an initial guess. The resulting

Table 1
Components in the thermal-hydraulic model.

Number	Component	Quantity
1	Fill	n_t
2	Break	n_t
3	One-cell pipe	$2n_t$
	Power	1
4	Cartesian vessel	1
5	Cylindrical vessel	1
	Heat structure bypass	n_t
	Heat structure barrel	n_t
	Heat structure bundle	n_{assm}
6	Lower single junction	n_{assm}
7	Upper single junction	n_{assm}
	Sideways pipe	$2n_z(n_x - 2 + n_y - 2)$

Table 2
Junctions in the thermal-hydraulic model.

Number	Junction from	Junction to	Quantity
a	Fill	Inlet one-cell pipe	n_t
b	Inlet one-cell pipe	Cyl. vessel	n_t
c	Cyl. vessel	Outlet one-cell pipe	n_t
d	Outlet one-cell pipe	Break	n_t
e	Cyl. vessel	Lower single junc.	n_{assm}
f	Lower single junc.	Cart. vessel	n_{assm}
g	Cart. vessel	Upper single junc.	n_{assm}
h	Upper single junc.	Cyl. vessel	n_{assm}
	Cart. vessel	Sideways pipe	$2n_z(n_x - 2 + n_y - 2)$
	Sideways pipe	Cyl. vessel	$2n_z(n_x - 2 + n_y - 2)$

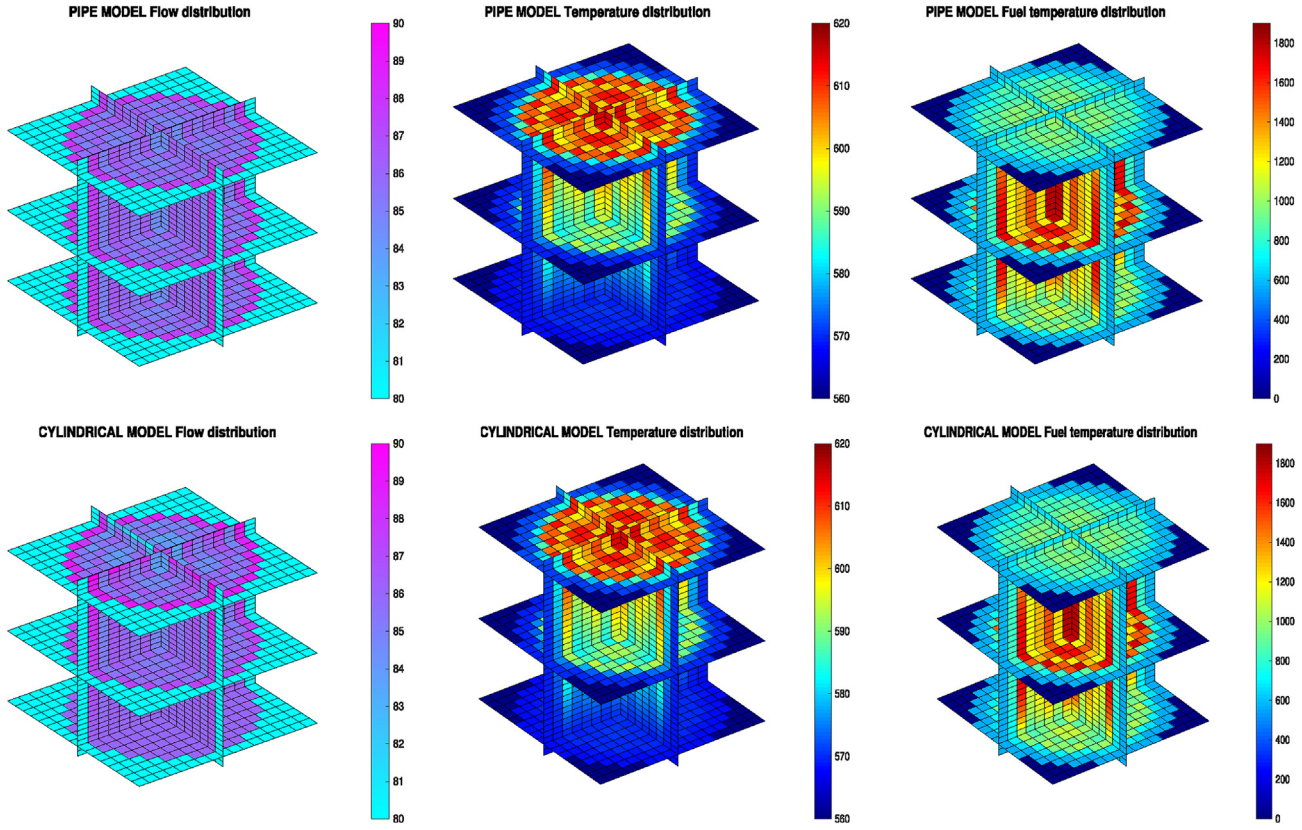

Fig. 3. Thermal-hydraulic model verification – 1D (PIPE) and 3D (CYLINDRICAL) model comparison.

bypass flow, $Flow_{by}$, is compared with the theoretical bypass flow, $Flow_{by}{}^{*}$. A correction factor based on the Darcy-Weisbach equation is applied to the axial bypass friction coefficients, $K_{by}{}^{Z}$, these are used in the next iteration. Note that each axial level may have a different friction coefficient, and thus, the correction is applied node-to-node. Only for 3D models, it is also possible to apply a correction for the radial bypass friction coefficients, $K_{by}{}^{R}$, for each axial level and theta sector. To decrease computational time, each new iteration is a restart case. The iteration process ends when the flow change between two consecutive iterations is smaller than a prefixed tolerance, ε_{flow}, defined by the user. In Fig. 4 a flow chart for the iterative process is presented, more information can be found in Ref. [16].

Where

i: iteration index,
z: axial node,
$\text{Flow}*_{\text{by}}$: theoretical bypass flow,
$\text{Flow}_{\text{by}}(i,z)$: simulated bypass flow for a given iteration and axial level,
ε_{flow}: flow tolerance limit,
$K^{Z}_{\text{by}}(i,z)$: axial bypass friction coefficient for a given iteration and axial level, and
$K^{R}_{\text{by}}(i,z)$: radial bypass friction coefficient for a given iteration and axial level.

The iterative process described above is successfully used to adjust the bypass flow for the 3D model presented in this work. Fig. 5 shows the comparison between bypass flow for the 3D model with three theta sectors (dashed lines) and the homologous 1D model (straight lines), note that the abscissa represents the axial axis. Due to the cross flow that exists in a real core, the flow

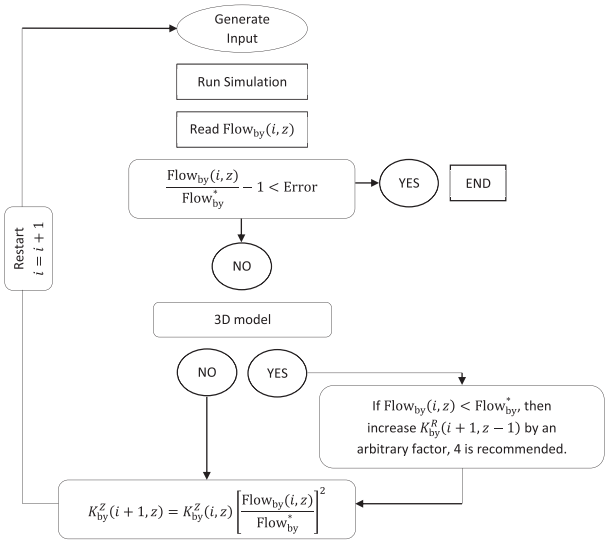

Fig. 4. Bypass friction coefficient adjustment iteration process.

represented by the 1D model is an average value, and the result given by the 3D model is the best-estimate flow. In this case, the tolerance limit is set to 5 kg/s, but any tolerance can be set.

2.2. Core model

A PWR is build with PARCS as a core model, its main characteristics are summarized in Table 3. The model contains 2 neutron energy groups and 6 delayed neutron groups. All boundary

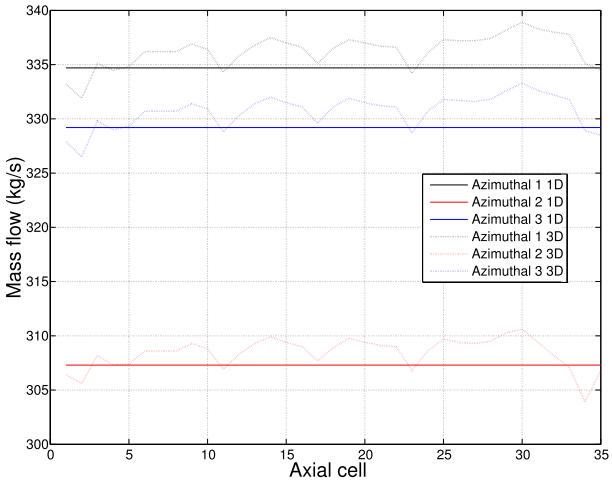

Fig. 5. Bypass flow comparison (axial direction) between 1D and 3D models.

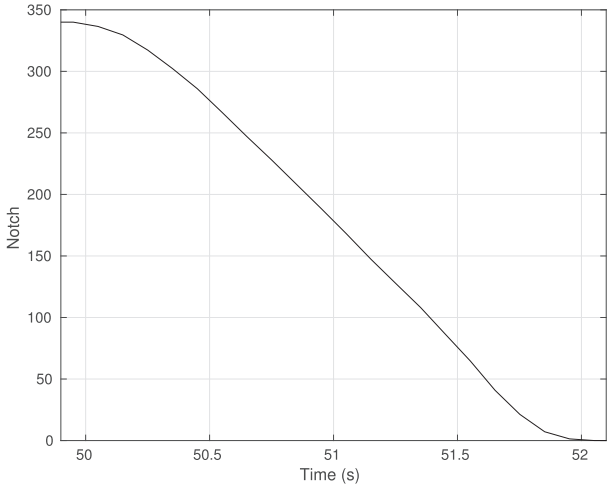

Fig. 6. Control rod insertion obtained from a real PWR test.

Table 3
Main features for the core physics model.

Property	Value
Power level	100%
Fuel assemblies	177
Assembly layout	16 × 16
Control rod banks	14
Radial cells	17 × 17
Axial cells	34 (2 refl.)
Cell dim. (cm)	23 × 23
Cell height (cm)	10.625
Fuel cells	177
Reflector cells	64
Fuel types	3
Neutronic comp.	1379 (3 refl.)

conditions are set to zero flux, thus all neutrons traveling outside the reflector are lost. The decay heat model is activated and the diffusion equation solver is HYBRID —recommended in PARCS manual—. The association between fuel assemblies and neutronic nodes is one to one —through MAPTAB file—, thus the model is not collapsed. The fuel type mapping and the control rod bank distribution are seen in Fig. 7. Besides, the neutronic library used to run the core physics code was obtained using SIMULATE3 following the SIMTAB methodology [17].

In addition, a control rod insertion —considered an *Anticipated Operational Occurrence* (AOO)— is simulated. PARCS code has a simple thermal-hydraulic model but, in this work, the neutronic model is coupled with the 3D thermal-hydraulic model (TRACE 5.0p3) described in Section 2.1. The rod insertion data corresponds to a real PWR test, the rod insertion movement can be seen in Fig. 6. The test is performed releasing a control rod —with maximum worth— from its lock and allowing its controlled fall, the reactor is operating at nominal power. Initially the control rod is fully withdrawn at notch 340. The insertion lasts 2.1 s and begins at 50.0 s. The whole simulation lasts 100.0 s, the purpose of the initial 50.0 s is to ensure that the initial conditions are properly converged. The control rod inserted is shown in Fig. 7 (right) as bank 14.

3. Methodology

The GRS methodology is used to propagate the thermal-hydraulic uncertainty through TRACE/PARCS coupled code. In this work only thermal-hydraulic macroscopic parameters are propagated, i.e. parameters that can be easily changed in a thermal-hydraulic code. The propagation of thermal-hydraulic microscopic parameters, such as local turbulence coefficients, or neutronic parameters, such as macroscopic cross sections, are out of the scope of this work. A total of 43 thermal-hydraulic parameters are selected to be propagated. Their PDFs definitions are found in the related literature or, if not found, defined based on expert judgment. These uncertainties are finally reflected on the enthalpy, power and reactivity predicted by PARCS. The U&S analysis is performed with DAKOTA 6.3 statistical tool.

The methodology is explained in detail in this section, the most important data is summarized in Table 4. Before going into details on the developed methodologies, a comment regarding the chosen sample size must be made. Since there are three dependent output parameters (power, reactivity and enthalpy), and only the upper tolerance region is of interest, the minimum sample size is 124 for a first order approach, see Eq (4). However, in this work, the chosen sample size is increased to 146.

The thermal-hydraulic uncertainty propagation through the thermal-hydraulic neutronic coupled code TRACE/PARCS is done using DAKOTA statistical tool. In total, 43 different input parameters are considered and two sampling methods (SRS and LHS) are compared. As output parameters, PARCS predictions for the enthalpy, power and reactivity are specified. These neutronic parameters are chosen because they represent the neutronic reactor state. Moreover, the enthalpy and reactivity (along with other parameters) define the safety limits for AOOs or postulated accidents [18]. The process to perform U&S analysis with DAKOTA can be summarized in five steps and is depicted in Fig. 8.

1. Define input parameters to be propagated and uncertainty PDFs for each of them. Ideally, these PDFs should be obtained experimentally and, if possible, expert judgment should be avoid.
2. Using these PDFs, 146 sets of perturbations are created with DAKOTA for each input parameter.
3. Using RESTING MATLAB program, 146 input decks for TRACE are created and a different perturbation set is applied to each input deck. An unperturbed case is also defined.
4. Run TRACE/PARCS coupled code for each input deck. Before the transient simulation, TRACE stand alone simulation is run to ensure a proper convergence.

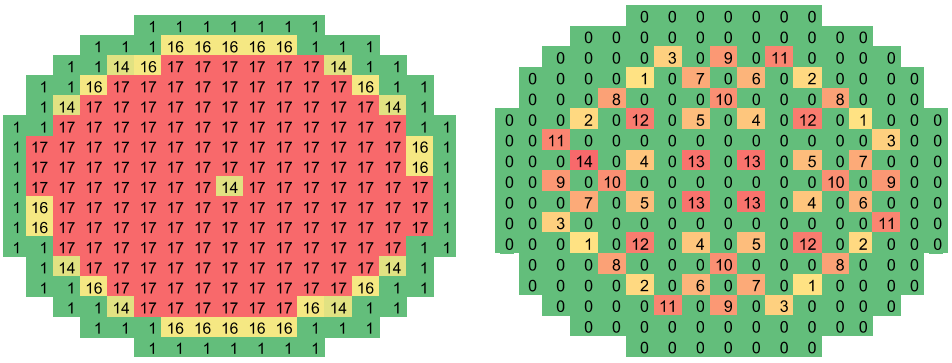

Fig. 7. Fuel type radial mapping (left) and control rod bank distribution (right).

Table 4
Data summary for thermal-hydraulic parameter uncertainty propagation.

Property	Value
Reactor	PWR
Code	TRACE5.0p3 & PARCSv3.0
U&S code	DAKOTA 6.3
Simulation state	SSA, CSS & CTR
Input parameters	Thermal-hydraulic parameters
Number of input param.	43
Output parameters	Power, enthalpy and reactivity
Number of output param.	3
Sampling method	SRS & LHS
PDF	Normal & Uniform

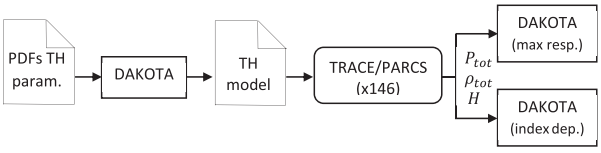

Fig. 8. Flow diagram for thermal-hydraulic parameter propagation.

5. Results for the different responses are gathered for the 146 transient simulations and DAKOTA is used to perform the U&S analysis.

3.1. U&S approach

Two different approaches are used to perform the U&S analysis, as explained in Ref. [3]. First approximation, or *maximum response approach*, calculates the U&S analysis only at time step where the maximum absolute response is found (for all responses). Thus, only one U&S analysis is run per output parameter. This approximation gives sensitivity information for the most critical transient time step. The second approximation, or *index dependent approach*, calculates the U&S analysis for each time step (whole simulation) and for all responses. The latter approximation gives sensitivity information for the whole transient simulation, thus, a wider sensitivity view for the analyst is obtained. The difference, between both approximations, lies in that different maximum responses are found —probably— at different time steps.

3.2. Input parameters

An extensive research in the literature is made in order to select the input parameters and characterize their uncertainty distributions. A list of thermal-hydraulic parameters is presented in Table 5 and Table 6 for normal and uniform distributions respectively. The parameters defining their PDFs are shown along with the references where the information is found. If PDF information is not found for a given parameter, expert judgment is applied. The same thermal-hydraulic parameter for different fuel types is considered as different input parameter but unchanged PDF. This PWR has three different fuel types —as shown in Table 3— plus the bypass, which has its own parameters. In total, 43 different thermal-hydraulic parameters are propagated.

It must be said that uncertainty information of parameters 32 to 43 are obtained in a BWR study and applied in a PWR in this work. It is expected that the uncertainty information for the friction factors and hydraulic diameters are similar for BWR and PWR. Regarding the gap heat transfer coefficients (parameters 32 to 35), even though it is know that its uncertainty information may differ for BWR and PWR, the BWR uncertainty data was applied as hypothesis (instead of using expert judgment) since this work only intends to demonstrate the viability of the methodology.

Uncertainty information for parameters representing boundary conditions (such as output pressure or inlet liquid temperature) must be chosen with caution. Thermal-hydraulic codes are very sensitive to boundary conditions. Even if all perturbed simulations finish successfully with a defined input uncertainty and sampling method, some simulations may fail with the same input uncertainty but another sampling method. Therefore, uncertainty definitions must suit all sampling methods. Normally, this is achieved performing an iterative process. In this work, it is found that SRS is more restrictive than LHS regarding uncertainty for boundary conditions.

4. Results

This section is splitted according to the followed approach (maximum response or index dependent).

4.1. Maximum response approach

Table 7 shows the average and the standard deviation —with the 95% *Confidence Interval* (CI)— for the output parameters (enthalpy, power and reactivity) for both sampling methods. The CI on the mean is calculated as Eq (8), where t_s is the inverse t-Student CDF with probability $1-\alpha$ and $n-1$ degrees of freedom. The sample size is n and s is the standard deviation of the sample. The CI on the standard deviation is calculated with Eq (9), where χ^2 is the inverse Chi-squared CDF with probability $1-\alpha$ and $n-1$ degrees of freedom. These equations must not be confused with Eq (3) or Eq (4) which give the minimum sample size (number of simulations) needed to cover the chosen output parameter domain with a

Table 5
Thermal-hydraulic parameters that follow a normal distribution.

#	Definition	Type	Variable	Mean	Std. deviation	Reference
1	Output pressure	–	P_{out}	1.0	0.002	Expert Opinion
2	Reactor power	–	q_{tot}	1.0	0.005	Expert Opinion
3	Inlet mass flow	–	m_{in}	1.0	0.001	Expert Opinion
4	Wall roughness	1	ε_1	1.0	0.25	Expert Opinion
5		2	ε_2			
6		3	ε_3			
7		Byp	ε_b			
8	Pitch to diameter ratio	1	p/d_1	1.0	0.05	Expert Opinion
9		2	p/d_2			
10		3	p/d_3			
11		Byp	p/d_b			
12	Assembly flow area	1	A_{flow1}	1.0	0.01	
13		2	A_{flow2}			[19]
14		3	A_{flow3}			page 13
15		Byp	A_{flowb}			
16	Radial fuel peaking factor	1	$RFPF_1$	1.0	0.01	
17		2	$RFPF_2$			[19]
18		3	$RFPF_3$			page 13
19		Byp	$RFPF_b$			

Table 6
Thermal-hydraulic parameters that follow a uniform distribution.

#	Definition	Type	Variable	Lower limit	Upper limit	Reference
20	Fuel heat capacity	–	Cp_{fuel}	0.99	1.01	[20], page 60
21	Clad heat capacity	–	Cp_{clad}	0.97	1.03	[20], page 60
22	Fuel thermal conductivity	–	K_{fuel}	0.954	1.046	[20], page 60
23	Clad thermal conductivity	–	K_{clad}	0.94	1.06	[20], page 60
24	Inlet flow temperature	–	T_{in}	−0.1	+0.1	[19] page 13/Expert
25	Critical heat flux multiplier	–	CHFM	−0.4	+0.3	[21] page 3.24
26	Bypass heat fraction	–	q_{byp}/q_{tot}	−2.375E-5	+2.375E-5	Expert Opinion
27	Moderator heat fraction	–	q_{mod}/q_{tot}	−9.263E-4	+9.263E-4	Expert Opinion
28	Gap size	1	z_{gap1}	−7.4E-6	+7.4E-6	Expert Opinion
29		2	z_{gap2}			
30		3	z_{gap3}			
31		Byp	z_{gapb}			
32	Gap heat transfer coefficient	1	h_{gap1}	0.65	1.35	
33		2	h_{gap2}			[22]
34		3	h_{gap3}			page 50
35		Byp	h_{gapb}			
36	Grid friction factor	1	k_{fac1}	0.95	1.05	
37		2	k_{fac2}			[22]
38		3	k_{fac3}			page 50
39		Byp	k_{facb}			
40	Hydraulic diameter	1	D_{hyd1}	0.995	1.005	
41		2	D_{hyd2}			[22]
42		3	D_{hyd3}			page 50
43		Byp	D_{hydb}			

Table 7
Comparing statistics for output parameters using SRS and LHS sampling methods.

Average	SRS	LHS
Enth. (J/kg)	2.63E+2 ± 8.27E-1	2.64E+2 ± 8.17E-1
Pow. (W)	9.12E-1 ± 6.19E-5	9.12E-1 ± 6.24E-5
Reac. ($)	−7.99E-2 ± 6.01E-5	−7.99E-2 ± 6.02E-5
Std. Dev.	**SRS**	**LHS**
Enth. (J/kg)	5.06E+0 ± 6.58E-1	5.00E+0 ± 6.50E-1
Pow. (W)	3.79E-4 ± 4.92E-5	3.82E-4 ± 4.96E-5
Reac. ($)	3.67E-4 ± 4.77E-5	3.68E-4 ± 4.78E-5

specified quantile α and probability β. The only relation between both terms is that as the minimum sample size is increased the confidence intervals will decrease.

$$CI_{\mu} = t_s \frac{s}{\sqrt{n}} \tag{8}$$

$$CI_{\sigma} = s\sqrt{\frac{n-1}{\chi^2}} \tag{9}$$

The histogram and scatter plot for the enthalpy (left) and reactivity (right) are seen in Fig. 9, both obtained with LHS sampling method. Besides, the SA for the power response is shown in Fig. 10, it contains the most sensitive input parameters for the power output parameter for both sampling methods LHS (left) and SRS (right). The most sensitive input parameters, for both sampling methods, are tabulated in Table 8. As shown in Eq. (5), an input parameter is considered to be sensitive enough if its *Partial Rank Correlation Coefficient* (PRCC) >0.1628. Input parameter

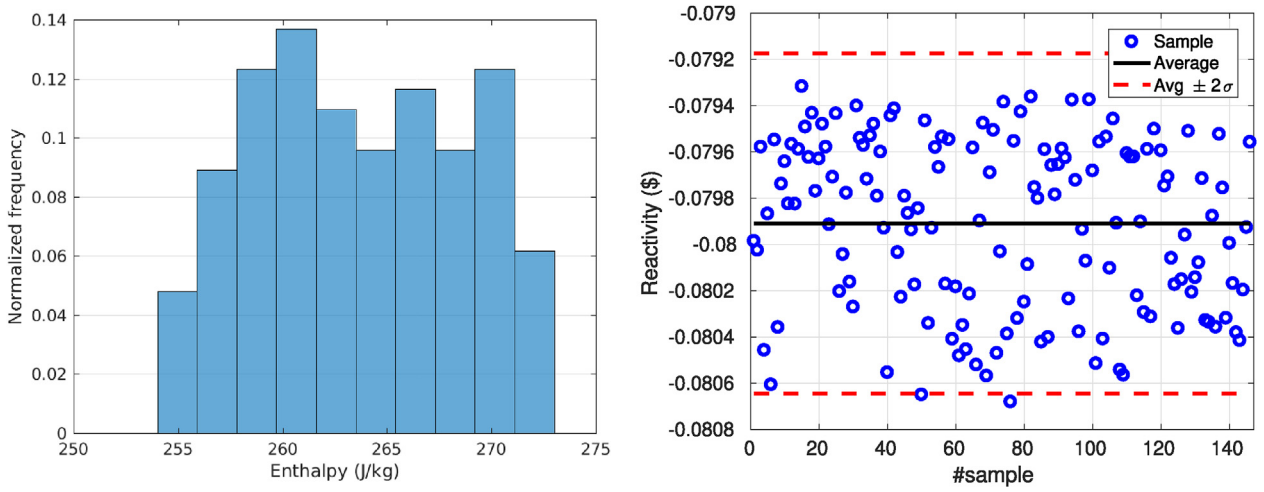

Fig. 9. Histogram for enthalpy (left) and scatter plot for reactivity response (right) when LHS is used for sampling the input parameters.

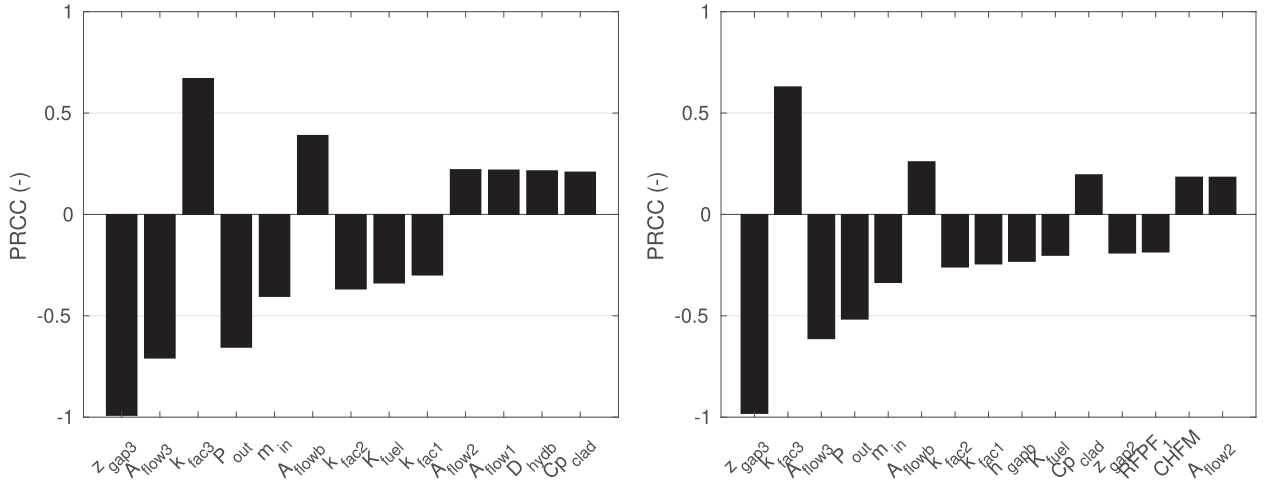

Fig. 10. PRCC between power and its most sensitive input parameters when the LHS (left) and SRS (right) methods are used.

Table 8
Ranking of most sensitive input parameters and their PRCC.

Enthalpy				Power				Reactivity			
LHS		SRS		LHS		SRS		LHS		SRS	
z_{gap3}	0.99	z_{gap3}	0.99	z_{gap3}	−0.99	z_{gap3}	−0.98	z_{gap3}	−0.99	z_{gap3}	−0.97
$p/\ d_3$	−0.68	p/d_3	−0.66	A_{flow3}	−0.71	k_{fac3}	0.63	A_{flow3}	−0.54	A_{flow3}	−0.51
$RFPF_1$	−0.21	T_{in}	0.22	k_{fac3}	0.67	A_{flow3}	−0.61	P_{out}	−0.47	P_{out}	−0.48
Cp_{clad}	−0.20	k_{fac3}	0.20	P_{out}	−0.66	P_{out}	−0.52	k_{fac3}	0.46	k_{fac3}	0.44
z_{gap2}	0.20	Cp_{clad}	−0.17	m_{in}	−0.40	m_{in}	−0.34	A_{flowb}	0.31	$RFPF_1$	−0.21
k_{fac3}	0.19			A_{flowb}	0.39	A_{flowb}	0.26	k_{fac1}	−0.23	k_{fac2}	−0.20
D_{hydb}	−0.18			k_{fac2}	−0.37	k_{fac2}	−0.26	m_{in}	−0.20	A_{flowb}	0.19
				K_{fuel}	−0.34	k_{fac1}	−0.24	k_{fac2}	−0.20	k_{fac1}	−0.18
				k_{fac1}	−0.30	h_{gapb}	−0.23	K_{clad}	0.17	CHFM	0.17
				A_{flow2}	0.22	K_{fuel}	−0.20	h_{gap1}	−0.17	Cp_{clad}	0.16
				A_{flow1}	0.22	Cp_{clad}	0.20				
				D_{hydb}	0.22	z_{gap2}	−0.19				
				Cp_{clad}	0.21	$RFPF_1$	−0.19				
						CHFM	0.18				
						A_{flow2}	0.18				

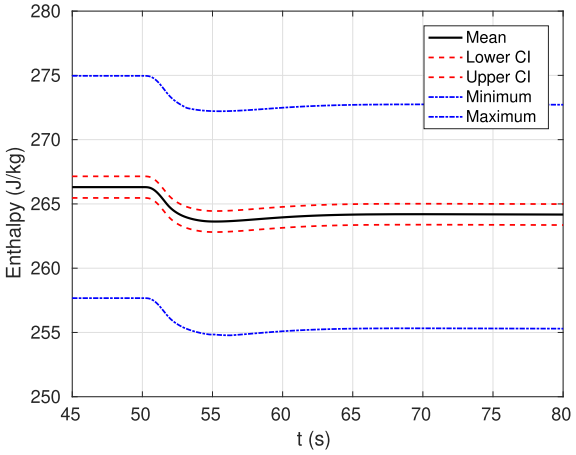

(a) Enthalpy average data, confidence interval and maximum/minimum response values.

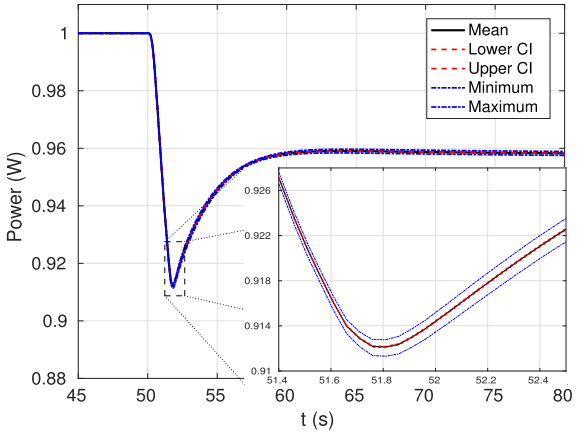

(b) Power average data, confidence interval and maximum/minimum response values.

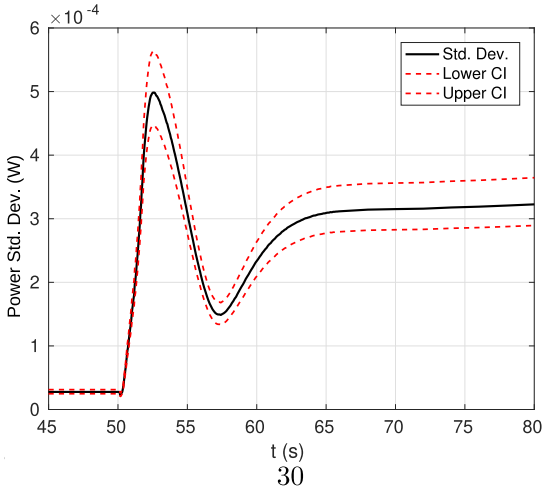

(c) Power standard deviation and confidence interval.

Fig. 11. Results for LHS method.

abbreviations and definitions can be found in Tables 5 and 6 for normal and uniform parameters respectively.

The conclusions extracted from Table 8 are that the fuel-clad gap size in assembly type 3 is always the most sensitive input parameter towards all output parameters and both sampling methods. The gap size has a positive PRCC for the enthalpy and negative PRCC value for the power and reactivity. On one hand, if the gap size is increased, the fuel temperature is also increased and thus, the enthalpy increases. On the other hand, due to the increase of fuel temperature and the Doppler effect, the absorption cross section is also increased and thus, the power and reactivity decreases. Regarding the power and reactivity, even though the order is different, the top four most sensitive input parameters are the same (regardless of the sampling method used). However, these are in disagreement with the most sensitive input parameters for the enthalpy. Moreover, there are further disagreements with the less sensitive input parameters. Sensitivity coefficients are expressed as the fraction of sensitivity apportioned by each input parameter. Therefore, the top sensitive input parameters make the biggest contribution to the uncertainty in output parameters. Other input parameters have little contribution and a little change —due to the sampling method used— could change the sensitivity ranking.

For both sampling methods, the assembly type 3 is always the assembly with more sensitive input parameters. Then assembly 2 and 1 are, roughly, equally sensitive, finally the bypass is the less sensitive. The great importance of input parameters belonging to assembly type 3 can be assessed using the fuel type distribution of Fig. 7. A great fraction of the core is represented using this assembly type (number 17 in that figure). Thus, a slight change in its definition affects the output parameters significantly. Mainly, the bypass does not have a great effect on the output parameters studied. The exception is the bypass flow area, which is significant enough, it greatly affects the core flow and thus the power and reactivity. The most sensitive boundary condition, for this case, is the outlet pressure for the power and reactivity followed by the inlet mass flow. Regarding the enthalpy, the most sensitive boundary condition is the liquid inlet temperature.

4.2. Index dependent approach

Fig. 11 shows the uncertainty results for the enthalpy and power responses as a function of time when LHS method is used. The results for the SRS method for the average and standard deviations are similar to the results presented in this section. This figure represents the average output parameter (solid black line), the lower and upper 95% confidence interval (dashed-red lines) and the maximum/minimum response value (dash-dot blue lines only for the average values). The total power response is normalized to one. A null transient of 50 s is run prior to the control rod insertion. It can be concluded that the most uncertain output parameter is the enthalpy, its biggest uncertainty is almost 2%. The uncertainty for the power and reactivity is 0.05% and 0.7% respectively. However, it must be said that the uncertainty for power and reactivity will be probably larger if other uncertainties were included, for example neutronic uncertainties.

Regarding the sensitivity analysis, Fig. 12 shows the PRCC values as a function of time for the power output parameter and LHS method. The results for the SRS method are also similar. A maximum of 14 most sensitive input parameters are shown. The results show that the most sensitive input parameter is, again, the gap size for the assembly type 3 —z_{gap3}—. In fact, it experience a great change in sensitivity when the AOO occurs (50 s) and it goes from a strong negative value to a strong positive value. Besides that, it is difficult to describe which are the most sensitive input parameters because PRCC values cross each other in time, hence the sensitivity ranking changes accordingly. The top three most sensitive parameters are the same for the power and reactivity (z_{gap3}, k_{fac3} and A_{flow3}), but different for the enthalpy (z_{gap3}, p/d_3 and z_{gap2} or T_{in}). Nevertheless, from Fig. 12, it is not clear the trend for the most sensitive boundary conditions. It seems that the outlet pressure is the most sensitive boundary condition for the LHS sampling method and that the inlet liquid temperature is the most sensitive for the SRS sampling method. Again, in general, little difference is shown between LHS and SRS sampling methods for the most sensitive input parameters, as concluded in Ref. [5].

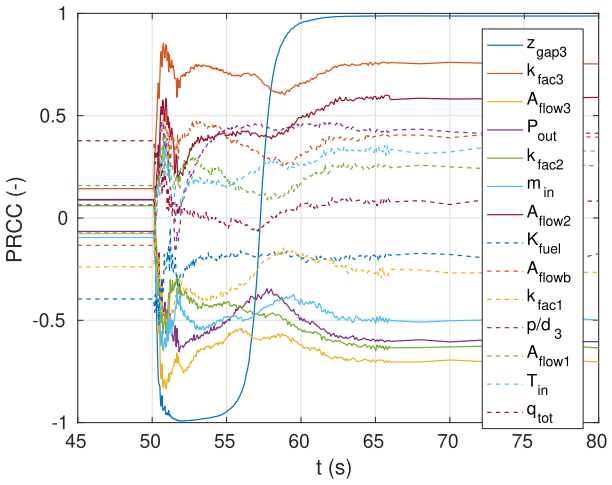

Fig. 12. PRCC as a function of time between power and its most sensitive input parameters when the LHS method is used.

5. Conclusions

This work presents the main results obtained with the GRS methodology to propagate the uncertainty of thermal-hydraulic parameters. The process covers one of the main phases of the benchmark released by the expert group on *Uncertainty Analysis in Modeling of Light Water Reactors* (UAM-LWR). The main innovative points achieved in this work are:

- Models. A new thermal-hydraulic model is developed with a highly-accurate 3D core discretization. Due to the 3D cross flow, bypass flow fluctuates strongly not only in the axial axis, but also among theta sectors. Therefore, an iterative process to adjust the bypass flow is presented in this work. A good agreement is obtained comparing the 3D model against a traditional 1D model.
- Real test. A control rod insertion is simulated with data obtained from a real PWR test.
- Software. RESTING MATLAB programs is developed to obtain highly-accurate thermal-hydraulic 3D core models and propagate the thermal-hydraulic uncertainty with DAKOTA.
- Methodology. Two approaches are used: *maximum response* and *index dependent*

The SA performed shows that the fuel-clad gap size is the most sensitive input parameter for both sampling methods: SRS and LHS. The sensitivity ranking follows with the assembly flow area, friction factors and pitch to diameter ratio. Discrepancies between LHS and SRS sampling methods are almost negligible. However, these can change the sensitivity ranking for medium and low sensitive input parameters. It is possible to know what is the most sensitive fuel type and therefore, the uncertainty of the model could be strongly

reduced if the uncertainty of this particular fuel type is reduced. Besides, parameters modeling the bypass are not especially sensitive with the exception of its flow area. This area mainly affects the power and the total reactivity (positive correlation). Extra care must be taken when assigning uncertainty information to the boundary conditions. The convergence of the simulation is greatly affected by its boundaries. Finally, it must be said that the use of expert judgment to assign uncertainty information should be avoided. Nonetheless, sometimes it is necessary due to the lack of uncertainty information.

Acknowledgement

The authors of this work thank the UAM-LWR benchmark organizers without whom this work would not have been possible. Besides, the authors sincerely thank to the Ministerio de Economía, Industria y Competitividad and the “Plan Nacional de I+D+i” for funding the projects NUC-MULTPHYS ENE2012-34585 and ENE2017-89029-P.

Appendix A. Supplementary data

Supplementary data to this article can be found online at https://doi.org/10.1016/j.net.2020.01.010.

References

[1] K. Ivanov, M. Avramova, S. Kamerow, I. Kodeli, E. Sartori, E. Ivanov, O. Cabellos, Benchmarks for Uncertainty Analysis in Modelling (UAM) for the Design, Operation and Safety Analysis of LWRs-Volume I: Specification and Support Data for Neutronics Cases (Phase I), Tech. Rep. (2013). Organisation for Economic Co-Operation and Development, Nuclear Energy Agency-OECD/NEA.

[2] M. Avramova, K. Ivanov, B. Krzykacz-Hausmann, K. Velkov, A. Pautz, Y. Perin, Uncertainty analysis of COBRA-TF void distribution predictions for the OECD/NRC BFBT Benchmark, in: Proceedings of the International Conference on advances in mathematics, computational methods, and reactor physics (M&C'09), 2009.

[3] C. Mesado, A. Soler, T. Barrachina, R. Miró, J. García-Díaz, R. Macián-Juan, G. Verdú, Uncertainty and sensitivity of neutron kinetic parameters in the dynamic response of a PWR rod ejection accident coupled simulation, Sci. Technol. Nucl. Install. (2012), https://doi.org/10.1155/2012/625878.

[4] A. Hernández-Solís, Uncertainty and Sensitivity Analysis Applied to LWR Neutronic and Thermal-Hydraulic Calculations, Ph.D. thesis, Chalmers University of Technology, 2012.

[5] G. Strydom, Uncertainty and sensitivity analyses of a pebble bed HTGR loss of cooling event, Sci. Technol. Nucl. Install. (2013), https://doi.org/10.1155/2013/426356.

[6] S. Wilks, Determination of sample sizes for setting tolerance limits, Ann. Math. Stat. 12 (1) (1941) 91–96.

[7] S. Wilks, Statistical prediction with special reference to the problem of tolerance limits, Ann. Math. Stat. 13 (4) (1942) 400–409.

[8] R. Macián-Juan, W. Tietsch, F. Sassen, Proposal for the Development and Implementation of an Uncertainty and Sensitivity Analysis Module in SNAP, US NRC NUREG/IA-0407, 2012.

[9] I. Hong, D. Oh, I. Kim, Generic Application of Wilks' Tolerance Limit Evaluation Approach to Nuclear Safety, 2013.

[10] I. Hong, A. Connolly, Generalized tolerance limit evaluation method to determine statistically meaningful minimum code simulations, in: 16th International Conference on Nuclear Engineering, American Society of Mechanical Engineers, 2008, pp. 653–660.

[11] L. Pal, M. Makai, Remarks on Statistical Aspects of Safety Analysis of Complex Systems, ArXiv Preprint Physics/0308086, 2002.

[12] A. Guba, M. Makai, L. Pál, Statistical aspects of best estimate method – I, Reliab. Eng. Syst. Saf. 80 (3) (2003) 217–232.

[13] W. Conover, Practical Nonparametric Statistics, third ed., John Wiley & Sons, Inc, 1999 third ed.

[14] C. Mesado, Uncertainty Quantification and Sensitivity Analysis for Cross Sections and Thermohydraulic Parameters in Lattice and Core Physics Codes. Methodology for Cross Section Library Generation and Application to PWR and BWR, Ph.D. thesis, Universitat Politècnica de València, 2017, http://hdl.handle.net/10251/86167.

[15] M. Garcıia-Fenoll, C. Mesado, T. Barrachina, R. Miró, G. Verdú, J.A. Bermejo, A. López, A. Ortego, Validation of 3D neutronic-thermohydraulic coupled codes RELAP5/PARCSv2.7 and TRACEv5.0p3/PARCSv3.0 against a PWR control rod drop transient, J. Nucl. Sci. Technol. (2017), https://doi.org/10.1080/00223131.2017.1329035.

[16] C. Mesado, R. Miró, T. Barrachina, G. Verdú, Modeling 3D Cores for PWR Using Vessel Components in TRACE v5.0P3 (NUREG/IA-0460), Tech. Rep, Universitat Politècnica de València (UPV), 2015.

[17] O. Roselló, Desarrollo de una metodología de generación de secciones eficaces para la simplificación del núcleo de reactores de agua ligera y aplicación en códigos acoplados neutrónicos termohidráulicos, Ph.D. thesis, Universitat Politècnica de València (UPV), 2004.

[18] US-NRC, et al., reportStandard Review Plan for the Review of Safety Analysis Reports for Nuclear Power Plants: LWR Edition - Transient and Accident Analysis, NUREG-0800.

[19] A. Petruzzi, F. D'Auria, Thermal-hydraulic System Codes in Nulcear Reactor Safety and Qualification Procedures, Science and Technology of Nuclear Installations.

[20] B. Boyack, R. Duffey, G. Wilson, P. Griffith, G. Lellouche, S. Levy, U. Rohatgi, W. Wulff, N. Zuber, Quantifying Reactor Safety Margins: Application of Code Scaling, Applicability, and Uncertainty Evaluation Methodology to a Large-Break, Loss-Of-Coolant Accident (NUREG/CR-5249), Tech. rep., Nuclear Regulatory Commission, Div. of Systems Research, Washington, DC (USA), 1989.

[21] T. Wickett, F. D'Auria, H. Glaeser, E. Chojnacki, C. Lage, D. Sweet, A. Neil, G. Galassi, S. Belsito, M. Ingegneri, et al., Report of the uncertainty method study, Tech. Rep. I (97) (1998) 35. OECD/CSNI Report NEA/CSNI/R.

[22] I. Gajev, Sensitivity and Uncertainty Analysis of Boiling Water Reactor Stability Simulations, Ph.D. thesis, 2012.